Periodic attention operates faster during more complex visual search

Garance Merholz[1]*, Laetitia Grabot[1], Rufin VanRullen[2], Laura Dugué[1,3]

[1]Université de Paris, INCC UMR 8002, CNRS, F-75006 Paris, France
[2]Université de Toulouse, CerCo UMR 5149, CNRS, F-31059 Toulouse, France
[3]Institut Universitaire de France (IUF), Paris, France
*gmerholz@gmail.com

Abstract

Attention has been found to sample visual information periodically, in a wide range of frequencies below 20 Hz. This periodicity may be supported by brain oscillations at corresponding frequencies. We propose that part of the discrepancy in periodic frequencies observed in the literature is due to differences in attentional demands, resulting from heterogeneity in tasks performed. To test this hypothesis, we used visual search and manipulated task complexity, i.e., target discriminability (high, medium, low) and number of distractors (set size), while electro-encephalography was simultaneously recorded. We replicated previous results showing that the phase of pre-stimulus low-frequency oscillations predicts search performance. Crucially, such effects were observed at increasing frequencies within the theta-alpha range (6-18 Hz) for decreasing target discriminability. In medium and low discriminability conditions, correct responses were further associated with higher post-stimulus phase-locking than incorrect ones, in increasing frequency and latency. Finally, the larger the set size, the later the post-stimulus effect peaked. Together, these results suggest that increased complexity (lower discriminability or larger set size) requires more attentional cycles to perform the task, partially explaining discrepancies between reports of attentional sampling. Low-frequency oscillations structure the temporal dynamics of neural activity and aid top-down, attentional control for efficient visual processing.

Introduction

Covert attention selects task-relevant stimuli among the constant flow of sensory information (in the absence of eye and head movement) to facilitate their processing [1-3]. A large literature (for review [4-8]) shows that spatial attention samples visual information periodically at low frequencies, i.e., < 20 Hz [9-19] and that this sampling is supported by brain oscillations at corresponding frequencies [20-24]. Critically, the frequencies reported in the literature show fairly large discrepancies (Table 1), which to date remains understudied. One parameter that may be involved is attentional demand, as it was shown to correlate with neural activity in posterior and frontal areas [44], visual neuronal activity [45], and with individual alpha peak frequency [46]. Here, we explicitly tested whether the variability in frequencies reported across the attentional sampling literature may be due to varying attentional demands, potentially caused by the disparity of tasks.

Study	**Frequency (Hz)**	**Measure**	**Range of tested frequencies (Hz)**	**Oscillation timing**
Non-human primate				
Visual search				
Buschman & Miller (2009)[25]	18-34	LFP phase dependence in FEF	18-34	whole trial
Cueing				
Voloh et al. (2015)[26]	~7	LFP phase dependence in ACC and PFC	4-29	post-cue
Fiebelkorn et al. (2018)[22]	~3.5 and 5 4, 12 and 28 (in LIP); 5, 10 and 21 (in FEF)	Oscillation in behavior (accuracy) LFP phase dependence in FEF and LIP	0-12 3-60	post-cue & pre-target post-cue & pre-target
Kienitz et al. (2018)[27]	~2-9 ~2-9	Oscillation in behavior (reaction times) MUA phase dependence in V4	2-12 2-12	post-stimulus
Fiebelkorn et al. (2019)[28]	5	LFP phase dependence in Pulvinar	3-60	pre-target
Gaillard et al. (2020)[29]	3-5 and 9-14 (accuracy) ~5-19 (reaction times) 7-12	Oscillation in behavior (accuracy & reaction times) Decoding score of cued location in MUA activity in PFC	1-16 (accuracy) 0-30 (reaction times) 0-55	post-cue & pre-target post-cue & pre-target
Zareian et al. (2020)[30]	8	LFP phase dependence in MT	8	post-cue & pre-target

Human				
Visual search				
Dugué & VanRullen (2014)[12]	2-3 and 9-10	Oscillation in behavior (accuracy)	2-20	post-stimulus onset
Dugué et al. (2015a)[20]	5.7 4-7 (pre-stimulus); 5.2-7.8 (post-stimulus)	Oscillation in behavior (accuracy) with TMS modulation of V1 activity EEG phase dependence	2.9-20 2-100	pre- and post-stimulus pre- and post-stimulus
Dugué et al. (2015b)[15]	2.4 and 7.1	Oscillation in behavior (accuracy)	2.4-16.7	post-stimulus
Dugué et al. (2017)[17]	2.4 and 4.8 (conjunction); 11.9 (feature)	Oscillation in behavior (accuracy)	2.4-14.3	post-stimulus
Dugué et al. (2019)[31]	4.5-7.3 and 17.6-18.3 (TMS over V1); 5-8.3 (TMS over FEF)	Oscillation in behavior (accuracy) with TMS modulation of V1 and FEF activity	2-38	post-stimulus
Cueing				
VanRullen et al. (2007)[9]	5.3-10	Modeling of behavioral accuracy	1-20	pre-target offset
Busch & VanRullen (2010)[32]	4-10	EEG phase dependence	2-50	post-cue & pre-target
Landau & Fries (2012)[10]	3.5-4.12 (right, target at cued location); 4.12-4.8 (right, uncued); 6.2-7.45 (left, cued); 9.4-9.95 (left, uncued)	Oscillation in behavior (accuracy)	0-30	post-cue & pre-target
Fiebelkorn et al. (2013)[33]	~3.5-5.5 (between objects); ~7-9 (within objects)	Oscillation in behavior (accuracy)	2-12	post-cue & pre-target
Song et al. (2014)[13]	8-20, modulated at 3-5 when valid and invalid trials are contrasted	Oscillation in behavior (reaction times)	0-25	post-cue & pre-target
Huang et al. (2015)[14]	~4	Oscillation in behavior (reaction times)	0-20	post-mask & pre-target
Landau et al. (2015)[21]	4	MEG brain rhythm (lateralized gamma band activity between hits and misses)	2-12	pre-target
Samaha et al. (2015)[34]	9-13	EEG brain rhythm	9-13	pre-target

Dugué et al. (2016)[16]	5 (invalid condition)	Oscillation in behavior (sensitivity d')	2.5-10	post-target & pre-TMS pulse
Chen et al. (2017)[35]	0.5, 1, 4, 6.6, 7, 19 (difficult task); 19.5 (easy)	Oscillation in behavior (accuracy)	0-25	post-cue & pre-target
Chen et al. (2018)[36]	6.25–8.59 in cued position and 1.56–2.34 in uncued (not dichoptic); 12.5-13.28 for both positions (dichoptic)	Oscillation in behavior (accuracy)	0-25	post-cue & pre-target
Harris et al. (2018)[37]	4-6 and 7-15 (cued target); 4-5 and 11-15 (uncued target)	EEG brain rhythm (phase opposition between detected and undetected target)	2-40	post-cue & pre-target
Helfrich et al. (2018)[23]	4.0 ± 0.9 (expe 1) 4.1 ± 1.3 (expe 2) ~4	Oscillation in behavior (accuracy) ECoG rhythm in electrodes responsive to cue	2-10 2-32	post-cue & pre-target post-cue
Senoussi et al. (2019)[18]	3.5-4 (attentional reorienting); 10-11 (perceptual sampling)	Oscillation in behavior (difference of probability of reporting the probe at most attended vs. at least attended location)	0.5-12	post-target & pre-probe
Peters et al. (2020)[38]	6	Oscillation in behavior (reaction time)	1.5-13.5	post-cue & pre-target
Balestrieri et al. (2021)[39]	5.1 (high attentional allocation); 7.4 (low attentional allocation)	Oscillation in behavior (accuracy)	0-13	post-cue & pre-target
Michel et al. (2021)[19]	4.8 (guess in combined valid and invalid trials); 9.6 (precision, in invalid trials only)	Oscillation in behavior (guess and precision from mixture models)	1.2-12	post-cue & pre-target
Plöchl et al. (2021)[40]	~4 ~4	Oscillations in behavior (accuracy) EEG brain rhythms	2-10 2-12	post-cue & pre-target post-cue
Re et al. (2019)[41]	~2.5-6 (two features); ~6.5-7.5 (single feature)	Oscillation in behavior (accuracy)	1-12	post-stimulus
van der Werf et al. (2021)[42]	7-8.3 (non-cued location for a cue 80% valid) – null results at cued location	Oscillation in behavior (accuracy)	2-10	post-cue & pre-target

van Es et al. (2021)[43]	4 and 17-20 (right FEF); 8-11 (right parietal cortex); 10-18 (left FEF); 4 and 8-12Hz (left parietal cortex)	MEG brain rhythm	4-20	post-stimulus onset (during stimulus presentation)

Table 1. Studies demonstrating periodic phase effects during covert visual attention tasks in human and non-human primates. *These studies were the "Attention and search" studies in VanRullen (2018)[96] and updated based on a literature search (until January 2022). The same criteria were used to select the studies, i.e., studies explicitly manipulating covert visual attention and showing a link between instantaneous phase and behavioral performance (from these studies, we only report results regarding oscillations in behavior, as well as analyses linking instantaneous neural phase and behavioral performance). Studies "entraining" brain oscillations were not included (see VanRullen, 2018[96], for more details). Properties of the periodicity are organized by species (non-human primate or human) and nature of the attentional manipulation (visual search or cueing; no other manipulation was found). Within these fields, the following sub-fields are included, from left to right: Study (chronological order); Frequency of significant rhythm (some of these values were not clearly reported in the publication and thus correspond to estimations based on Figure reading; indicated with ~); Measure used in the study to reveal periodicity; Range of all tested frequencies; Oscillation timing relative to trial events. Note that the table does not include negative findings. LPF: Local Field Potential. FEF: Frontal Eye Field. ACC: Anterior Cingulate Cortex. PFC: Lateral Prefrontal Cortex. LIP: Lateral Intraparietal Area. MUA: Multi-Unit Activity.*

Visual search tasks — looking for a target among distractors — have been largely used to study attention (for review [47,48]), and more specifically its temporal dynamics. A periodic attentional mechanism implies cycles of discrete sampling windows over time. Visual search is particularly adapted to test the link between these attentional cycles, neural oscillations and task demands, because task demands may be easily manipulated by varying target discriminability among distractors or varying the number of distractors.

It has been proposed that attentional sampling during visual search tasks relies on periodic neural activity [5,7,20,49,31]. Particularly, it was shown that the pre- and post-stimulus phase of theta oscillations (4-8 Hz) distinguished correct from incorrect trials [20]. Interestingly, when disrupting low-level occipital (V1) or high-level attentional (FEF) areas in humans using transcranial magnetic stimulation (TMS), performance was modulated periodically at low frequencies (< 20 Hz) [20,49,31]. In other words, specific delays at which TMS was administered during the task led to increased behavioral performance while others led to decreased performance, with preferred and unpreferred delays alternating periodically at low frequencies. This result was interpreted as evidence that the sampling process of attentional selection during visual search is periodic and is supported by brain oscillations at low frequencies. It is also consistent with hierarchical models of visual search, which posit that effortful search involves iterative communication between occipital

and frontal areas [50-53]. Such an iterative process may be subtended by corresponding low-frequency neural oscillations [5,7,20,49,31,54].

Here, we recorded electro-encephalography (EEG) during visual search tasks with varying attentional load to test the link between brain oscillations and task demands, and further characterize periodic attentional sampling. We first replicated previous results showing that pre-stimulus phase [20,32,55-63] and post-stimulus phase-locking across trials [20,64,65] of low-frequency oscillations predict successful task performance (same task as in [20]). Specifically, the phase of spontaneous oscillations (before stimuli onset) predicts trial outcome; and post-stimulus phase alignment (phase-locking) aids performance, which we call phase reset here to refer, strictly, to the mathematical description of the effect [66].

The novelty in the present study lies in the implementation of a gradient of task demands during visual search in two separate experiments. Crucially, we tested the prediction that an increase in the number of cycles required to perform the search would result in an increase in the frequency of the underlying neural oscillations, and/or in a delayed peak of the neural response. Specifically, we manipulated the discriminability of the target (Experiment 1) and the number of items in the search array, i.e., set size (Experiment 2). Our working hypothesis was that during one attentional cycle only a limited amount of information from the search array is processed – either because not all stimuli are attended at once, or because attention is divided among all stimuli and thus less resources are attributed to each stimulus (here, we do not aim to disentangle these two options). It follows that given a fixed search duration, the more complex the search task, the higher the frequency of the neural oscillation required for successful performance – allowing more cycles to be completed in the same amount of time. Moreover, alpha/theta phase realignment has been associated with more efficient sensory processing of targets [20,30]. Therefore, if lower discriminability and additional items entail more attentional cycles, and if phase-locking aids performance while processing the target, a delayed phase reset can be expected, to allow for a periodic sampling process to cycle through the search array and complete the processing of the target.

In Experiment 1, the target and distractors' shapes were manipulated to obtain three levels of discriminability (high, medium and low, with equalized task performance; blocked). We tested two predictions: (1) the lower the discriminability, the higher the frequency of the pre- and post-stimulus brain oscillations underlying attentional performance; (2) the lower the discriminability and the later the optimal phase reset, resulting in delayed post-stimulus temporal dynamics. Indeed, some phase resetting is to be expected simply due to stimulus onset [66,67], but a stronger reset should lead to better performance [20], hence higher phase-locking is expected in correct trials. Furthermore, if the search requires on average more attentional cycles, as hypothesized when increasing search complexity, then this would translate in an optimal phase reset that appears at a delayed latency.

In Experiment 2, the set size (number of items in the search array, 4 or 8; interleaved) was manipulated. Here, we tested a last prediction: (3) the optimal phase reset affecting behavior occurs at a delayed latency and higher frequency when more items are presented (i.e., higher task complexity). Because the participant cannot predict the set size of the upcoming trial, we did not expect an effect of set size on pre-stimulus activity and thus did not test it – there is no reason to assume here that participants can adapt their sampling frequency in advance.

Altogether, the results confirm our three predictions and suggest that increased attentional demands requires more attentional cycles to perform the task (higher frequency), partially explaining discrepancies between reports of attentional sampling.

Results

Behavior

Participants performed a visual search task with varying parameters while electroencephalography (EEG) was simultaneously recorded (Fig. 1). In Experiment 1, the effect of discriminability between target and distractors was tested with three conditions (high, medium, and low discriminability; blocked). We titrated the stimulus-onset asynchrony (SOA) for each participant to ensure that their percentage of correct responses remained around 70% and to minimize task difficulty differences between conditions (mean SOA ± SD: high = 40 ± 5 ms, medium = 82 ± 13 ms, low = 271 ± 26 ms; Fig. 1B). Participants' performance across all conditions was on average at 66% (SD = 6%, ranging from 55 to 85%, Fig. 1C). For the high discriminability condition, average performance was at 68 ± 8%, 68 ± 9% for medium, and 61 ± 6% for low discriminability. A one-way repeated-measures ANOVA revealed that the percentage of correct responses in Experiment 1 significantly differed between discriminability conditions ($F(1,2) = 3.73$, $p = 0.034$, $\eta^2 = 0.18$). Post-hoc 2-by-2 t-tests revealed that performance in the low discriminability condition was significantly lower than in the high and medium discriminability conditions (see Statistics Table 1). There was no significant difference in performance between the high and medium conditions.

Condition comparison	*p*	CI	t	df	Cohen's d
high vs. low discriminability	< 0.01*	[2.1, 11.9]	3.11	11	0.98
medium vs. low discriminability	< 0.001*	[4.3, 10.7]	5.13	11	0.98
high vs. medium discriminability	0.854	[-6.3, 5.3]	-0.19	11	-0.06
4 vs. 8 items	0.008*	[1.7, 9.0]	3.27	10	1.06

Statistics Table 1. Performance comparisons (2-by-2 t-tests) between experimental conditions. **: significant p values. CI: 95% Confidence Interval. df: degrees of freedom.*

In Experiment 2, the effect of set size was tested with either four or eight items presented (interleaved) in the search array (medium discriminability items were used). The SOA was titrated to minimize task difficulty differences between conditions (mean SOA ± SD: 4 items = 69 ± 43 ms, 8 items = 129 ± 78 ms, Fig. 1B). The average performance across both conditions was at 79% (SD = 4, ranging from 65 to 90 %, Fig. 1C). For the 4-items condition, average performance was at 81 ± 4%, and 76 ± 5% for 8 items. A two-tailed t-test showed that performance was significantly lower in the 8-items condition compared to the 4-items condition (see Statistics Table 1). The medium discriminability condition in Experiment 1 and the 4-items condition in Experiment 2 exhibited the same items and set size, and a two-tailed heteroscedastic t-test revealed that their SOAs were comparable ($p = 0.189$). However, their performance levels were significantly different ($p < 0.0001$), perhaps due to inter-individual differences or to item placement on the screen (Fig. 1A).

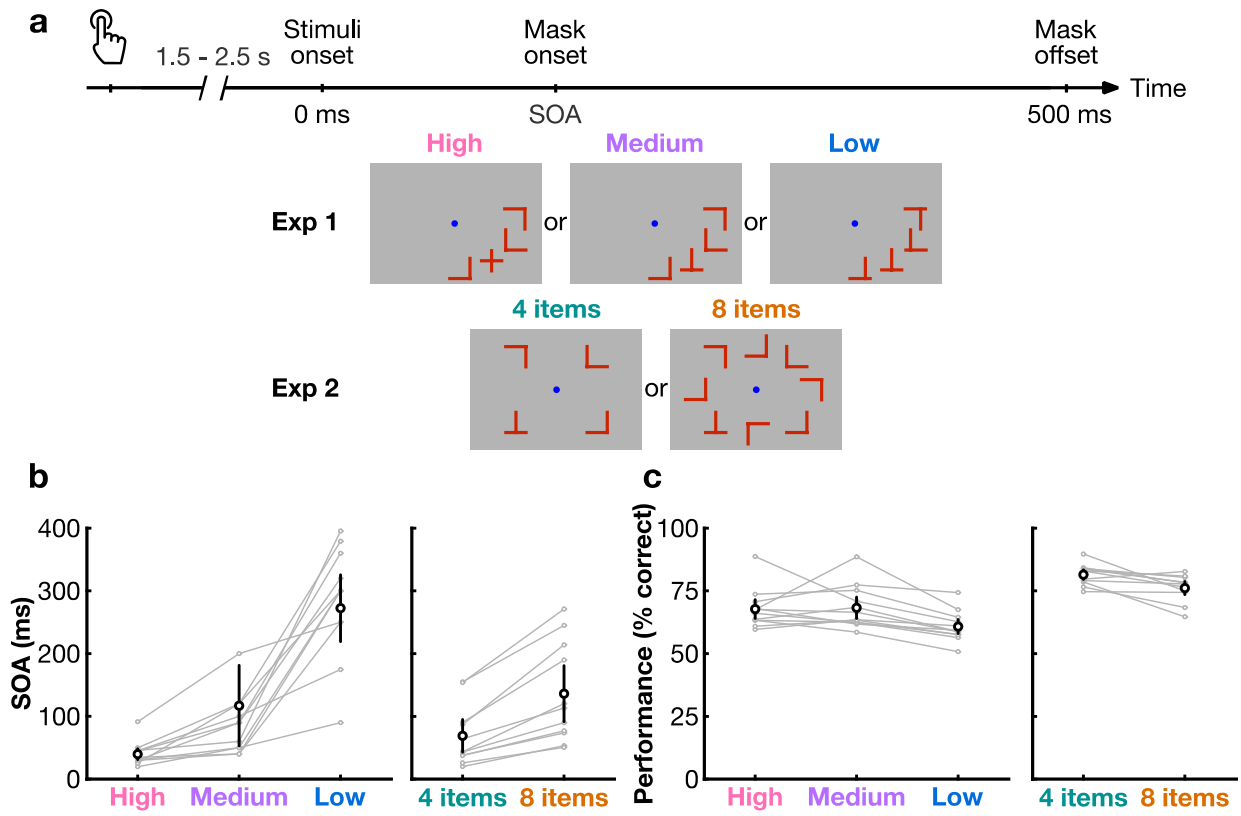

Figure 1. Task design and behavioral results. *(**a**) A button press initiated by the participant began the trial. After a random duration between 1.5 and 2.5 seconds, the search array appeared. In Experiment 1, the item shape was manipulated (blocked) to yield high (the target is a +), medium and low (the target is a T) discriminability conditions (always 4 items). In Experiment 2, the number of items was manipulated (4 or 8, interleaved; the target is always a T). The items remained onscreen for the duration of the participant's titrated SOA, immediately followed by masks, which disappeared after 500 ms from stimuli onset. After mask offset, the participant pressed a button to indicate whether the target was present or absent, ending the trial. The central fixation dot was always present. (**b**) Stimuli duration (SOA) for Experiment 1 (left) and Experiment 2 (right) for each condition. (**c**) Performance expressed as the percentage of correct responses (detecting the presence or absence of the target). Black circles represent the group average performance. Error bars represent the 95% confidence interval. Gray traces show results for individual participants.*

Pre-stimulus phase impacts performance at increasing frequency with lower discriminability

We first tested the prediction that the lower the discriminability, the higher the frequency of the pre-stimulus brain oscillations underlying attentional performance. Phase opposition sum (POS) [20,62,68,69] values were estimated for each frequency, pre-stimulus time point and discriminability condition in Experiment 1. A positive POS indicates that the phase is locked in correct trials and that it is locked in the opposite direction in incorrect trials (see Materials and Methods). An FDR-

corrected permutation test showed a significant phase opposition between correct and incorrect trials at low frequencies (i.e., 6.6-14.3 Hz; Fig. 2) for the three discriminability conditions. We observed that the peak frequency of POS rose with difficulty: 7 Hz for high, 9.7 Hz for medium and 10.6 Hz for low discriminability condition. The frequency band containing significant POS (blue outline in Fig. 2) had no overlap between the high discriminability condition (6.6 to 7.1 Hz) and the lower-discriminability conditions (medium: 8.5 to 11.1 Hz, low: 8.5 to 14.3 Hz). The topographies at POS peaks (marked by stars) showed that the effect was localized in the occipital and frontal poles (Fig. 2, bottom).

To ensure that the observed phase opposition effects were not spuriously generated by amplitude differences, we performed a similar analysis on amplitude. Although we observed significant differences between correct and incorrect trials (high: 8 to 12 Hz and -70 to 0 ms, medium: 6 to 17 Hz and -400 to -130 ms, low: 14 to 18 Hz at -200 ms, see Supplementary Material), these clusters did not overlap with those found for POS (Fig. 2) in the high and low discriminability conditions; the amplitude effects are thus unlikely to be merely due to amplitude differences. Note that there is partial overlap in the medium condition; we thus cannot completely rule out this interpretation for this condition.

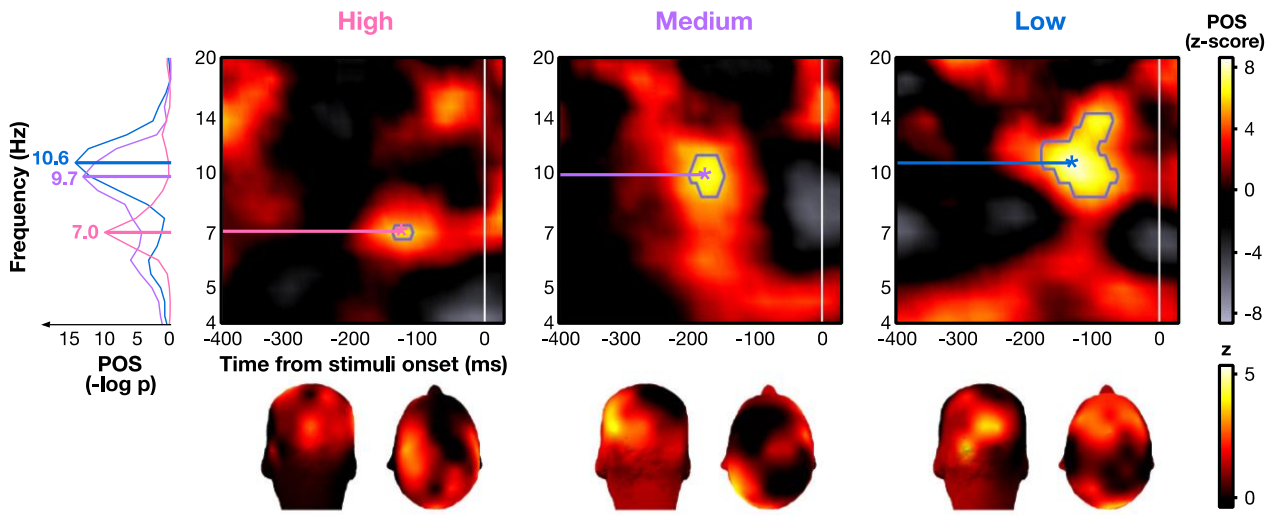

Figure 2. Pre-stimulus phase opposition between correct and incorrect trials in Experiment 1. *Z-score of pre-stimulus phase opposition sum (POS) of correct and incorrect trials for the high, medium and low discriminability conditions, combined across all electrodes and all participants. Blue contours indicate areas above the FDR threshold (alpha = 10^{-7}, corresponding to p value thresholds of 2.2e-10, 5.0e-10, and 4.7e-9 respectively). Stars indicate the time-frequency point of maximum significance (high: z_{max} = 6.42 at f_{max} = 6.96 Hz and t_{max} = -129 ms; medium: z_{max} = 7.49 at f_{max} = 9.75 Hz and t_{max} = -176 ms; low: z_{max} = 8.91 at f_{max} = 10.60 Hz and t_{max} = -137 ms). Topomaps represent the average POS (z-score) at each electrode across participants for the point of maximum significance, indicated by a star. The left panel plot shows the converted POS (-log p values) of the high, medium and low discriminability conditions (pink, purple and blue traces,*

respectively) at the timepoint with the maximum z-score (bootstrap-corrected POS in -log(p) of 10.17 for high, 13.48 for medium and 14.68 for low).

Post-stimulus phase-locking impacts performance only in complex searches

We tested the prediction that the lower the discriminability, the later the optimal reset of neural oscillations involved in attentional search, resulting in slower post-stimulus temporal dynamics. Post-stimulus phase-locking was compared between correct and incorrect trials. The analysis was restricted to the task-relevant frequency band found in the pre-stimulus analysis (from the lowest to the highest FDR-corrected significant frequencies, i.e., 6.6 to 14.3 Hz; Fig. 2). At each time point within each participant and condition, phase-locking difference (PLD) between correct and incorrect trials was averaged across the frequency band of interest. FDR-corrected permutation tests showed that the PLD was significantly different from zero only in lower-discriminability searches (medium: $p < 0.001$, 82 to 106 ms; low: $p < 0.01$, 184 to 270 ms), suggesting that correct trials were more phase-locked than incorrect trials in these conditions (Fig. 3A). PLD was not significantly different from zero in the high discriminability condition (p-values remained above the FDR threshold constrained by an alpha parameter of 0.01). The topographies represent the distribution of the activity at the point of maximum significance over all electrodes (Fig. 3A). Note that the effect in the medium condition is localized in fronto-occipital areas, while it is rather parieto-occipital in the low discriminability condition.

A two-tailed paired t-test showed that the PLD peaked at significantly different latencies between medium (mean ± sd: 188 ms ± 89 ms) and low (224 ms ± 73 ms) discriminability conditions (see Statistics Table 2; Fig. 3A). Since the latency difference between average peaks (140 ms) was close to the difference in average duration of stimuli presentation (SOA) for these two conditions (Δ_{SOA} = 190 ms, Fig. 1B), we investigated whether the PLD difference in latencies was due to the experimental design by calculating the correlation between individual PLD peak latency and average stimuli duration for each participant. No significant correlation was observed (see Statistics Table 3), suggesting that the delay in PLD latencies was not likely due to SOA differences.

If these post-stimulus phase-locking differences found here truly captured the phase reset of the pre-stimulus oscillation, they should show the same frequency dissociation observed in pre-stimulus activity between discriminability conditions. To test this prediction, the PLD at the timepoint of maximum significance of the average traces for the lower-discriminability search conditions (medium: 98 ms, low: 238 ms, stars in Fig. 3A) was plotted across frequencies (Fig. 3B). We observed that the PLD peaked in a significantly higher frequency for the low discriminability task than for the medium one (medium: 9.2 Hz ± 3.0 Hz, low: 14.0 Hz ± 3.6 Hz; see Statistics Table 2), and at similar frequencies as those observed for the pre-stimulus phase opposition. Note that the high discriminability condition is not shown because no timepoint survived the FDR-corrected permutation test in the frequency-band-average analysis (see Fig. 3A).

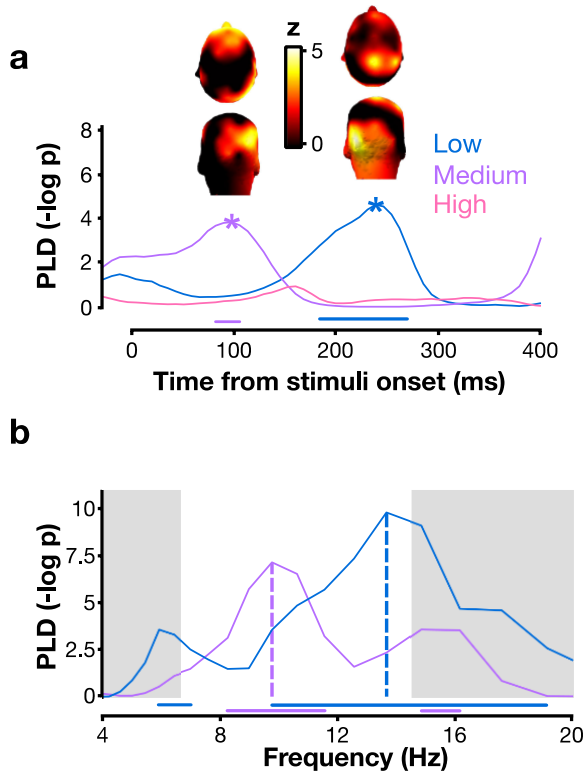

Figure 3. Post-stimulus phase-locking difference between correct and incorrect trials in Experiment 1. *(**a**) The phase-locking difference (PLD) is the difference in inter-trial phase coherence (ITC) between correct and incorrect trials. The PLD curves are plotted after averaging across the frequency range of the significant clusters found in pre-stimulus phase opposition (Fig. 2). Stars mark the timepoint of maximum significance on each trace (medium: 98 ms; low: 238 ms). Topomaps represent the PLD at each electrode averaged across participants at the timepoint of maximum significance. (**b**) PLD curves plotted at the timepoints of maximum significance against frequency for the medium (purple) and low (blue) discriminability conditions. The white area indicates the frequency range of interest, taken from the pre-stimulus phase opposition effect. On both panels, horizontal bars along the bottom indicate that the PLD of the corresponding curve (blue: low discriminability; purple: medium discriminability) is above the significance threshold corrected for multiple comparisons (FDR).*

Condition comparison	*p*	CI	t	df	Cohen's d
medium vs. low peak latency	0.010*	[30, 171]	3.28	8	1.14
medium vs. low peak frequency	0.009*	[1.5, 8.0]	3.3	9	1.37
4 vs. 8 items peak latency	0.030*	[12, 190]	2.56	9	1.30
4 vs. 8 items peak frequency	0.12	[-1.2, 7.8]	1.75	7	0.91

Statistics Table 2. Comparisons between PLD peaks (two-tailed paired t-tests). *Same conventions as in Statistics Table 1.*

Condition	r	*p*	CI
Medium discriminability	-0.23	0.532	[-0.63, 0.83]
Low discriminability	-0.32	0.330	[-0.85, 0.52]
4 items	0.18	0.596	[-0.62, 0.80]
8 items	0.12	0.741	[-0.69, 0.80]

Statistics Table 3. Correlation between individual PLD peak latency and average stimuli duration in each experimental condition. *CI: 95% Confidence Interval.*

Adding items increases the delay of the post-stimulus phase-locking effect

In Experiment 2, the number of items in the search array was manipulated (4 or 8; interleaved). Since participants could not predict the set size of the upcoming trial, we did not test for pre-stimulus frequency effects. Here, we specifically hypothesized that more attentional cycles would be required after stimulus onset if the number of items to process increased, leading to a higher frequency (for the same period of time) and/or a delayed response due to a delay in the post-stimulus phase-locking. We first contrasted the post-stimulus phase-locking between correct and incorrect trials for combined 4- and 8-items conditions. The FDR-corrected permutation test showed that post-stimulus phase-locking value was higher in correct than incorrect trials between 10.2 Hz and 16.9 Hz (FDR $p < 1e-8$, Fig. 4A). The significant clusters showed a fronto-occipital topographical distribution, similar to the topographies observed in Experiment 1 (Fig. 3A).

We then investigated this effect for each item-number condition separately. We restricted this analysis to the frequency band impacting behavior by averaging the PLD between 10.2 Hz and 16.9 Hz. We found a significant effect of phase-locking on performance in both conditions (4 items: $p < 0.01$, significant cluster from 20 to 293 ms; 8 items: $p < 0.001$, significant cluster from 184 to 270 ms; Fig. 4B). Critically, we observed that the 8-items condition was associated with a

273 significantly later peak than the 4-items condition (4 items: 113± 92 ms; 8 items: 223 ± 61 ms; see
274 Statistics Table 2). As in Experiment 1, we calculated the correlation between stimuli duration
275 (SOA) and peak timing to check whether the timing difference could be due to the experimental
276 design. We did not find any significant correlation (see Statistics Table 3), suggesting a dissociation
277 between PLD latencies and SOA. The topographies taken at the points of maximum significance
278 (marked by stars on Fig. 4B) showed that the phase effect is fronto-occipital in both item-number
279 conditions.

280 Last, we investigated whether the phase-locking difference occurred at different frequencies
281 according to the item condition. We plotted the PLD at the timepoints of maximum significance (4
282 items: 137 ms; 8 items: 238 ms) against frequency for the two conditions separately (Fig. 4C).
283 Similarly as for Experiment 1 (Fig. 3B), when more items were presented, a trend toward a higher
284 frequency was apparent (4 items: 9.6 Hz ± 4.2 Hz; 8 items: 13.7 Hz ± 2.9 Hz), although this effect
285 was not significant (see Statistics Table 2).

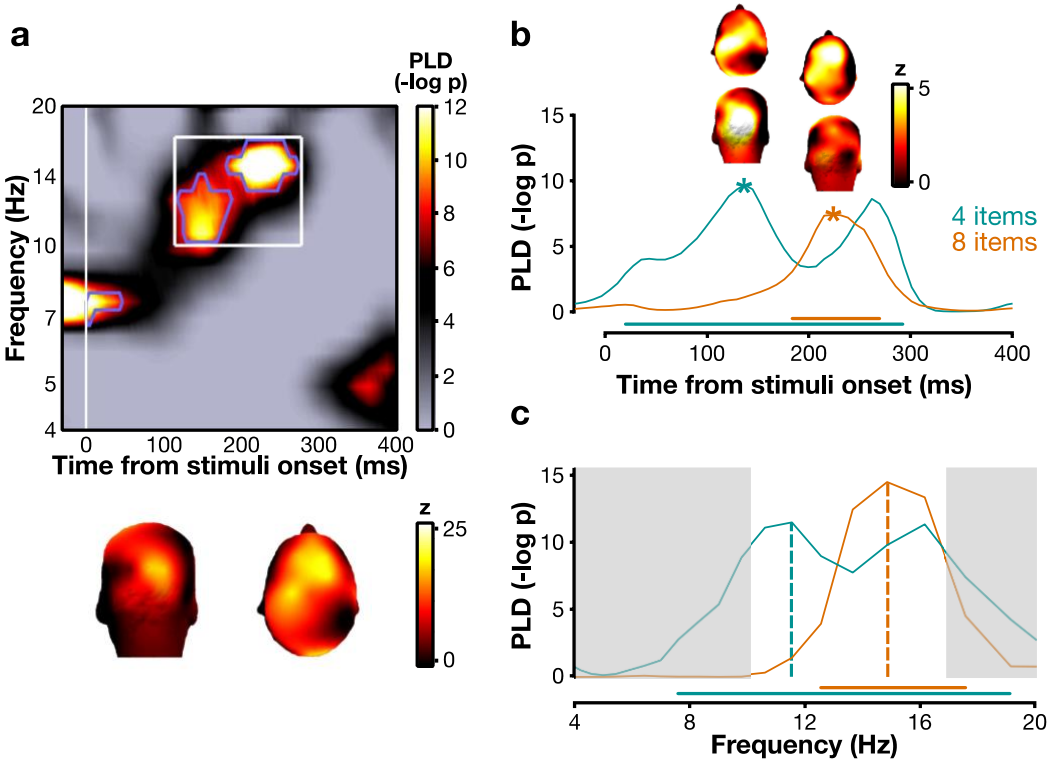

286

287 ***Figure 4. Post-stimulus phase-locking difference between correct and incorrect trials in***
288 ***Experiment 2.*** *(**a**) P value of post-stimulus phase-locking difference (PLD) between correct and*
289 *incorrect trials for both conditions combined (4 and 8 items), pooled across all electrodes and all*
290 *participants. Blue contours indicate areas above the FDR threshold (alpha = 10^{-7}, corresponding to*
291 *a p value of 4.4e-9). The bottom topomaps represent the average activity across participants for*
292 *the time-frequency area within the bounds of FDR-corrected significant blue contours (white*
293 *rectangle: 114 to 277 ms and 10 to 17 Hz). (**b**) PLD curves plotted after averaging across the*

*frequency range of the significant clusters found in (a). Stars mark the timepoint of maximum significance on each trace (4 items: 137 ms; 8 items: 238 ms). Topomaps represent the PLD at each electrode averaged across participants at the timepoint of maximum significance. (**c**) PLD curves plotted against frequency at the timepoint of maximum significance for the 4-item (teal) and 8-item (orange) condition. On both panels, the horizontal bars along the bottom indicate that the curves surpass the FDR threshold (correction for multiple comparisons). The white area indicates the frequency range of interest, taken from the significant PLD clusters in (a).*

Discussion

The frequency of attentional sampling reported across the literature shows large discrepancies [4-24]. We propose that part of this heterogeneity is due to inconsistent attentional demands across tasks. The aim of this study was to investigate the link between brain oscillations and attentional demands as manipulated by the discriminability of the target and the set size in a visual search task. We replicated previous findings showing that 7-10 Hz pre-stimulus phase distinguishes correct from incorrect responses [20,32,55-63]. The novelty of the present study lies in the finding that this phase opposition effect is concentrated in rising frequency with degraded discriminability. This link between frequency and discriminability was also found in the post-stimulus phase-locking difference between correct and incorrect search trials. A second independent dataset revealed a similar pattern between the frequency of this post-stimulus phase-locking difference and the number of presented items. Finally, we found significant latency effects of the post-stimulus phase-locking impacting performance both when discriminability was degraded and when distractor number was increased.

We interpret the results under the framework of hierarchical models of visual search. Most theoretical accounts of attentional search propose that lower-level visual areas iteratively communicate with higher-level areas (e.g., [50-53]). Top-down signaling would redirect attention toward candidate items, thus amplifying specific visual neuronal populations consecutively until the target is found. It has been proposed that hierarchical frameworks of visual search involving iterative communication between lower- and higher-level brain regions rest on periodic neural activity in these regions [5,7,20,31,49], possibly involving a causal temporal structuring of visual cortex activity by FEF [70]. If the iterative communication suggested by attentional search models can only process a limited number of items at each iteration, and the time allotted for the search is limited (as in the current experiments), then the frequency should increase with search complexity (lower discriminability or higher set size) to complete more iterations within the same time window. Our results concur with this model, which constitutes the most parsimonious explanation for our findings.

Experiment 1 shows that the less discriminable the target is among the distractors, the higher the frequency of pre-stimulus phase opposition between correct and incorrect searches. This

suggests that the neural system can adjust to an optimal frequency, based on goal-directed expectations. Specifically, the frequencies of interest in the high discriminability condition showed no overlap with those in the medium and low discriminability conditions (Fig. 2). However, there was overlap between the medium and low conditions, suggesting that the increase in frequency is not linear across discriminability conditions. This non-linear increase may be related to unequal differences in task demands between conditions, which are difficult to quantify, or to real non-linearity between frequency and task demands. Further investigation is thus needed to distinguish between these two possibilities. A similar frequency modulation was found in the post-stimulus phase-locking effect: the difference in post-stimulus phase coherence between correct and incorrect responses follows increasing frequency with degraded discriminability, as does the pre-stimulus phase effect. This frequency increase is also observed in Experiment 2 (although without reaching the statistical threshold), where trial types were interleaved (i.e., the viewer could not know in advance whether they would search among 4 or 8 items). Together, these results clearly point to a direct link between specific task complexity and brain oscillations. Following hierarchical models' predictions, this may indicate that the more iterations are performed to find the target, the more neural cycles are generated in the same constrained time window, in line with the hypothesis that more attentional iterations between frontal and occipital regions are implemented through neural oscillations. Our findings are consistent with a previous study, which found that the peak frequency of alpha oscillations involved in a visual discrimination task decreases when the task requires temporal integration relative to temporal segregation (block design) [71]. In the present study, integration could be beneficial for a partially pop-out visual task, such as the high discriminability condition (L vs. +), while temporal segregation would allow processing of more demanding visual searches, potentially requiring sequential processing of stimuli in the search array [25,72,73]. This frequency modulation of pre-stimulus spontaneous oscillations may be controlled by a dynamic top-down signal adjusting to task demands [7,31,34,71,74,75]. One can speculate that a feedback signal gives rise to the lower frequency phase effect found in the high discriminability search condition, thus integrating the search items and facilitating attentional capture by the salient target. A higher frequency in lower-discriminability conditions could, however, enhance segregation between items and contribute to their sequential processing.

The present results show that the phase effects are localized in both low-level (occipital) and frontal regions, which is also coherent with an integration-segregation dissociation mediated by top-down signals. Previous research suggests that the dorsolateral prefrontal cortex (dlPFC) facilitates attentional orienting towards target-like stimuli and comparison between the currently attended stimulus and the target [25,76]. Additionally, oscillations in the frontal eye fields (FEF) are involved in attention shifts [8,25,76]. The theta rhythm was reported to gate and regulate the connections between these anterior and posterior areas [5-7]. Coherent with these previous findings, we observed that the pre-stimulus phase opposition effect is localized over frontal and occipital electrodes for medium and low discriminability, whereas there is minimal frontal contribution in the

high discriminability search condition (Fig. 2, bottom). Moreover, the activity in occipital electrodes decreases when there are more items, leaving mainly frontal activity (Fig. 4B). Consistent with a recent study showing minimal involvement of occipital rhythms during an attentional task [77], our observations suggest that frontal areas are more strongly recruited under more complex (difficult) search conditions. Previous literature on exogenous (involuntary) and endogenous (voluntary) attention has shown that exogenous attention relies on bottom-up signals while endogenous attention relies on top-down ones [75,78-84]. Similarly, here, easier search tasks (high discriminability and small set size) may preferentially involve automatic, bottom-up perceptual capture, while more difficult tasks (lower discriminability or large set size) may involve top-down attentional deployment. Indeed, the features that distinguish target (+) and distractors (Ls) in the high discriminability condition are likely to trigger bottom-up attentional capture [85]. Bottom-up signals may be supported by higher frequency bands (hardly recordable using EEG) compared to top-down mechanisms, such as gamma oscillations [86,87]. This limitation can explain the absence of lower-frequency effects in post-stimulus phase-locking in the highly-discriminable, partially exogenous search (Fig. 3A) as well as the absence of frontal involvement in this condition (Fig. 2). Our results therefore suggest that a top-down control tuning the frequency of neural oscillations aids performance in difficult searches.

The results further show that the post-stimulus phase coherence difference between correct and incorrect responses is delayed with increasing complexity (lower target discriminability or larger set size). The mask delay onset, which was adjusted for each participant and condition, could potentially have confounded this effect. Yet, we found no correlation between stimuli duration and peak delay, which argues against this possibility. This is consistent with a previous study using a similar design [20], which found that periodic behavioral modulation was not dependent on stimulus duration during a visual search, and that the onset of the mask did not evoke any performance modulation. We interpret the delayed effect in the framework of two-stage hierarchical models of visual search, i.e., when search tasks are more complex, more iterations between the sensory and the attentional stages are necessary, which is supported by more neural cycles. Such a mechanism implies that the optimal phase reset – leading to the strongest phase-locking – will occur later on average compared to less complex search tasks. Further studies will investigate whether the reset may only affect search while processing the target. Finally, one might notice some discrepancies between effect localizations (Fig. 3): both the low and medium discriminability conditions showed an occipital effect, but while the low condition showed also a frontal activation, the medium condition showed a parietal one. This difference might be explained by the involvement of different brain areas, hence explaining the different delays of the effect between the two conditions. It might also come from differences in dipoles within similar brain areas, which can project differently onto the sensors. Further investigation is thus warranted.

This study contributes to filling the missing experimental evidence for the current models of attentional search and provides novel support for a link between brain oscillations and attentional demands, which may be a factor to explain the frequency variability observed in the literature. Our results suggest that brain oscillations support attentional sampling, which may correspond to the iterations posited by biologically-plausible computational and cognitive models of attentional search. Importantly, the pre-stimulus modulation of frequency, accompanied by post-stimulus frequency and latency modulations in the same direction, indicate a capacity for low-frequency oscillations (< 20 Hz) to structure the temporal dynamics of neural activity and aid top-down, attentional control for maximally efficient visual processing.

Materials and Methods

Participants

Thirteen participants (6 women) were recruited for Experiment 1. One was excluded from analyses because they were not able to maintain fixation. Thirteen different participants (5 women) were recruited for Experiment 2. Two were excluded due to poor EEG signal quality. All participants (age between 18 and 35 years) had normal or corrected-to-normal vision and declared no previous history of neurological disorders or diagnoses. All participants provided written informed consent and received monetary compensation for their time. The study followed the principles prescribed by the declaration of Helsinki and was approved by the ethics committee "CPP Sud-Ouest et Outre-Mer I," under protocol number 2009-A01087-50.

Apparatus and Stimuli

Both experiments were conducted in a dark room, with the participant sitting 57 cm away from a CRT monitor (800x600 pixels; refresh rate: 140 Hz), their head positioned using a chinrest. The stimuli were red letter-like symbols (oriented randomly 0°, 90°, 180° or 270° from vertical) and masks (squares barred by a cross of the same size as the stimuli) presented away from a central fixation dot on a uniform gray background, created under the MATLAB software (The MathWorks, www.mathworks.com, version R2016b) using the Psychophysics Toolbox [88-90].

In Experiment 1, the shape of the stimuli was manipulated. Four stimuli (1.8° x 1.8° visual angle) were presented simultaneously, either on the lower right or lower left quadrant of the screen (randomly), at a fixed eccentricity (8°). In the high discriminability condition, the distractors were L shapes and the target was a + shape. In the medium condition, the distractors were L shapes and the target was a T shape. In the low discriminability condition, the distractors were distorted L shapes with the horizontal bar slightly shifted up so they resembled a T, and the target was a T shape (Fig. 1A).

In Experiment 2, the set size was manipulated. The distractors were always L shapes and the target a T shape. In the 4-items condition, four stimuli were presented at 8° of eccentricity (one

443 at each of the cardinal positions around fixation), and in the 8-items condition, eight stimuli were
444 presented: one at each cardinal position and one at each diagonal position around fixation (Fig.
445 1A).
446
447 **Experimental Procedure**
448 *Behavioral pre-test for Experiment 1*
449 To assess the discriminability of items in the attentional search task for each condition, the
450 participants from Experiment 1 (not Experiment 2) first performed a behavioral pre-test at the
451 beginning of the experimental session testing the three different stimuli shapes (L vs. +, L vs. T or
452 distorted-L vs. T) and the two set sizes (4 or 8 items). Trials in this behavioral pre-test were blocked
453 by shape condition (104 trials per shape), with the two set sizes pseudorandomly interleaved in
454 every block (52 trials per set size in each block). Participants were instructed to report as fast as
455 possible whether the target was present or absent in the array, and the stimuli stayed present on
456 the screen until the participant pressed a response key (left arrow for target present, and right arrow
457 for absent). A t-test on median reaction times shows a weak but significant difference between 4
458 and 8 for L vs. + items (4 items: 548 ± 46 ms, 8 items: 580 ± 48 ms, median ± 95% CI, $p = 0.0058$,
459 CI = [-29,-6], $t(10) = -3.50$). There is a greater difference between 4 and 8 items with L vs. T (4
460 items: 591 ± 52 ms, 8 items: 759 ± 75 ms, median ± 95% CI, $p < 0.0001$, CI = [-144,-71], $t(10) = -$
461 6.51) and with distorted-L vs. T (4 items: 1696 ± 224 ms, 8 items: 2426 ± 408 ms, median ± 95%
462 CI, $p < 0.0001$, CI = [-1208,-672], $t(10) = -7.81$). Crucially, the reaction times are significantly more
463 increased as discriminability decreases (L vs. +: Δ_{RT} median ± 95% CI = 22 ± 10 ms; L vs. T: 131
464 ± 32 ms; distorted-L vs. T: 1052 ± 236 ms; t-test of L vs. + against L vs. T: $p < 0.001$, CI = [-129,-
465 51], $t(10) = -5.18$; L vs. + against distorted-L vs. T: $p < 0.0001$, CI = [-1192,-653], $t(10) = -7.63$; L
466 vs. T against distorted-L vs. T: $p < 0.0001$, CI = [-1089,-576], $t(10) = -7.23$). We therefore label the
467 L vs. + condition as a high discriminability condition, the L vs. T as medium and the distorted-L vs.
468 T as low discriminability. We selected the stimuli shape from the medium discriminability condition
469 (L vs. T) for Experiment 2, in which we then manipulated set size.
470
471 *EEG sessions*
472 In both experiments, at each trial, participants were asked to fixate a central dot. Their eye
473 position was verified a posteriori using the electro-oculography (EOG) signal, and only trials with
474 no blink nor saccade were kept for the analyses (mean ± sd: 158 ± 50 rejected epochs). Participants
475 began each trial by pressing a key. After a random temporal jitter of 1.5 to 2.5 seconds, the stimuli
476 appeared on the screen for the duration of the Stimulus-mask Onset Asynchrony (SOA) defined for
477 each individual, and were directly followed by masks, for a total duration of 500 ms. The SOA was
478 titrated for each participant and each condition in a preliminary staircase block with an adaptive
479 staircase procedure [91] to obtain an average performance level of 70% correct responses. The
480 SOA was re-adjusted after each block if necessary, to maintain this level throughout the

experiment. The average SOA across all participants was 40 ± 5 ms (SD) for the high discriminability, 82 ± 13 ms for the medium, and 271 ± 26 ms for the low discriminability condition in Experiment 1; and 69 ± 43 ms for the 4-items condition and 129 ms ± 78 for the 8-items condition in Experiment 2. The target was present randomly on half of the trials. Participants were asked to report whether the target was present or absent as accurately as possible, without a time limit. Participants reported the presence or absence of the target using a keyboard (right arrow key for present and left arrow key for absent). All participants used their right hand.

In Experiment 1, participants performed 6 blocks (2 of each discriminability condition) in pseudorandomized order across participants, with 250 trials per block, leading to 500 trials per condition in total. In Experiment 2, the set size conditions (4 items or 8 items) were pseudorandomly interleaved within the blocks. Participants performed 30 blocks with 40 trials per block, leading to 600 trials per condition in total. The total experiment duration varied between 2 and 2.5 hours to account for the EEG setup, the behavioral pre-test (for Experiment 1), the staircase procedure (for both Experiments 1 and 2), and breaks.

Behavioral analyses and statistics

The behavioral dependent variable was participants' percentage of correct responses, which was aimed to be maintained at 70% to ensure that participants were not guessing the answer and that there was a balanced ratio of correct and incorrect trials. A trial was labeled as correct if the participant correctly identified that a target was present or correctly reported that the target was absent. Trials which were rejected in EEG pre-processing were also deleted from the behavioral analysis. Conditions were compared using a repeated-measures one-way ANOVA in Experiment 1 (three conditions) and two-tailed t-tests (post-hoc in Experiment 1). The present study was not designed to measure differences between target-present and target-absent conditions, and therefore does not include sufficient numbers of trials in these constrained cases [68]. Future experiments are needed to investigate this difference.

In the pre-test for Experiment 1, the principal dependent variable was the reaction time (measured between stimulus onset and the participant's response) as a function of the number of stimuli in the search array (4 or 8). This was measured for each level of discriminability (high, medium and low). Only the trials in which participants gave a correct response were included in the analysis. This pre-test enabled us to compute the difference between median reaction times (Δ_{RT} or slope) for 4 vs. 8 items, and thus to measure how strongly the number of distractors affected performance, independently for each shape condition. The reaction times when 4 or 8 items were presented, and the slopes for each shape condition, were compared using pairwise (2-by-2) t-tests.

EEG acquisition and pre-processing

EEG was recorded using a 64-electrode ActiveTwo Biosemi system. Two extra electrodes, Common Mode Sense (CMS) and Driven Right Leg (DRL) were used as reference and ground.

They were placed on the participant's face, with CMS on the left cheek and DRL on the right. Eye movements were recorded with EOG using three additional electrodes: one on each side of the eyes (to record horizontal eye movements) and one under the right eye (to record vertical movements).

All EEG analyses were performed under MATLAB using the eeglab toolbox [92] and custom scripts. Numerical computations were partly performed on the S-CAPAD platform, IPGP, France. The data were downsampled to 512 Hz, re-referenced to the average over all electrodes, and epoched from -1500 to +1000 ms relative to search array onset. The data were cleaned by visual inspection to remove artifacts: large spurs of high-amplitude, high-frequency activity in one or more electrodes (muscle contractions), blinks and saccades, as made evident by a sharp depolarization and repolarization in the EOG (eye movements), slow drifts of large amplitude in more than 3 electrodes. In addition, electrodes were interpolated using spherical spline interpolation if they read noisy signal for more than 7 % of the trials. On average, 134 ± 20 (mean ± sd) epochs were rejected per participant (~9 %) in Experiment 1 and 182 ± 80 epochs in Experiment 2 (~15%). Epochs were then labeled according to performance (correct or incorrect) for each condition.

Phase and amplitude analyses

Time-frequency decomposition was performed using Morlet wavelets on single trials [93]. The wavelets' length evolved logarithmically from 3 to 6 cycles between 4 and 20 Hz. The signal was expressed at every time-frequency point as a complex vector. Inter-Trial phase Coherence (ITC; otherwise called phase-locking) was computed by averaging the complex exponentials over all trials of a given condition for each time-frequency point, electrode and participant. This analysis was done separately for correct and incorrect trials in each condition. To account for the imbalanced ratio of correct/incorrect trials (70%/30%), the correct trials were randomly subsampled to attain the same number as the incorrect trials (repeated 100 times).

To analyze whether the pre-stimulus phase between correct and incorrect trials differed, Phase Opposition Sum (POS) was computed at each time-frequency point:

$POS = ITC_{correct} + ITC_{incorrect} - 2*ITC_{all}$.

A low POS indicates that the two conditions (correct and incorrect) have random phase distributions, whereas a high POS means that phase-locking is strong in both conditions. The measure of POS accounts for uniform distributions of phases: to ensure that the phase was truly opposed between correct and incorrect trials, we checked for circular uniformity (Hodges-Ajne test) of the phase angles (see [68,69]) across all trials (characteristic of a spontaneous signal) at the point of maximum significance at sensor Oz, because it is activated in the 3 conditions (high, medium and low discriminability; see Fig. 2), and ensured that no instance of non-uniformity was found (high discriminability: p = 0.242, kappa = 0.3; medium: p = 0.854, kappa = 0.148; low: p = 0.92, kappa = 0.037). Therefore, a strong phase-locking in one condition presupposes a phase-locking in the other condition in opposite phase, and thus a high POS [52].

We also measured post-stimulus Phase-Locking Difference (PLD) between correct and incorrect trials, defined as: PLD = $ITC_{correct} – ITC_{incorrect}$. A high PLD reveals a strong phase-locking for correct trials and a weak phase-locking for incorrect trials, meaning that one precise phase for the reset aided performance (correct trials), and trials resetting away from this ideal phase led to low performance on average (incorrect trials). As mentioned in the introduction, the term “reset” is used here purely to refer to the mathematical description of the resulting signal.

Using the time-frequency decomposition by Morlet wavelet described above, the amplitude for each time-frequency point was also computed by taking the length of each complex vector. Baseline correction was applied by subtracting the mean value from -0.4 to -0.1 s from stimulus onset. The same subsampling procedure as for the ITC calculation was performed.

The POS and PLD significance was tested using a permutation procedure. Following the null hypothesis according to which there is no difference between correct and incorrect trials, we compared the averaged phase-locking values to shuffled surrogates of the data within each participant. The surrogates were generated by shuffling “correct” and “incorrect” trial labels while keeping the original number of incorrect trials and subsampling correct trials as described above. This procedure was repeated 10,000 times to obtain a null distribution. The POS and PLD were converted to a z-score, by subtracting the mean of the null distribution (shuffled surrogate) from the real POS or PLD, and dividing by the null distribution's standard deviation. This yielded a z-score for each participant, which were then combined using the Stouffer method [68,94] to obtain a group-level z-score. This z-score was expressed as a p-value using the cumulative distribution function. Multiple comparisons were corrected using the False Discovery Rate (FDR) procedure, in which the p-values associated with each time-frequency point are ordered and thresholded [95], with a threshold α value of 10^{-7}. To test for the presence of outliers in the data, a leave-one-out procedure was performed wherein one participant at a time was removed from the pool.

These analyses were performed from -0.4 to 0 s (around search array onset) for the POS and 0 to 0.4 s for the PLD. The same statistical procedure was applied to amplitude. Finally, individual participants peak values POS, and PLD were compared across experimental conditions. Participants that did not exhibit any significant POS or PLD peak individually were excluded from the comparison analyses (in Experiment 1, three participants were excluded from the latency comparison and two from the frequency comparison, resulting in a total n of 9 and 10, respectively; in Experiment 2, one participant was excluded from the latency comparison and three from the frequency comparison, resulting in a total n of 10 and 8, respectively).

Data Availability

The datasets generated during and/or analyzed during the current study are available from the corresponding author upon reasonable request.

References

1. Brefczynski, J. A. & DeYoe, E. A. A physiological correlate of the ‘spotlight’ of visual attention. *Nat. Neurosci.* **2**, 370–374 (1999).

2. Carrasco, M. Visual attention: the past 25 years. *Vision Res.* **51**, 1484–1525 (2011).

3. Posner, M. I. Attention: the mechanisms of consciousness. *Proc. Natl. Acad. Sci.* **91**, 7398-7403 (1994).

4. VanRullen, R. Perceptual cycles. *Trends Cogn. Sci.* **20**, 723–735 (2016).

5. Dugué, L. & VanRullen, R. Transcranial magnetic stimulation reveals intrinsic perceptual and attentional rhythms. *Front. Neurosci.* **11**, (2017).

6. Fiebelkorn, I. C. & Kastner, S. A rhythmic theory of attention. *Trends Cogn. Sci.* **23**, 87–101 (2019).

7. Kienitz, R., Schmid, M.C. & Dugué, L. Rhythmic sampling revisited: experimental paradigms and neural mechanisms. *Eur. J. Neurosci.* ejn.15489 (2021).

8. Gaillard, C. & Ben Hamed, S. The neural bases of spatial attention and perceptual rhythms. *Eur. J. Neurosci.* ejn.15044 (2020).

9. VanRullen, R., Carlson, T. & Cavanagh, P. The blinking spotlight of attention. *Proc. Natl. Acad. Sci.* **104**, 19204–19209 (2007).

10. Landau, A. N. & Fries, P. Attention samples stimuli rhythmically. *Curr. Biol.* **22**, 1000–1004 (2012).

11. Fiebelkorn, I. C. *et al.* Cortical cross-frequency coupling predicts perceptual outcomes. *NeuroImage* **69**, 126–137 (2013).

12. Dugué, L. & VanRullen, R. The dynamics of attentional sampling during visual search revealed by Fourier analysis of periodic noise interference. *J. Vis.* **14**, (2014).

13. Song, K., Meng, M., Chen, L., Zhou, K. & Luo, H. Behavioral oscillations in attention: rhythmic α pulses mediated through θ band. *J. Neurosci.* **34**, 4837–4844 (2014).

14. Huang, Y., Chen, L. & Luo, H. Behavioral oscillation in priming: competing perceptual predictions conveyed in alternating theta-band rhythms. *J. Neurosci.* **35**, 2830–2837 (2015).

15. Dugué, L., McLelland, D., Lajous, M. & VanRullen, R. Attention searches nonuniformly in space and in time. *Proc. Natl. Acad. Sci. USA* **112**, 15214–15219 (2015b).

16. Dugué, L., Roberts, M. & Carrasco, M. Attention reorients periodically. *Curr. Biol.* **26**, 1595–1601 (2016).

17. Dugué, L., Xue, A. M. & Carrasco, M. Distinct perceptual rhythms for feature and conjunction searches. *J. Vis.* **17**, 22 (2017).

18. Senoussi, M., Moreland, J. C., Busch, N. A. & Dugué, L. Attention explores space periodically at the theta frequency. *J. Vis.* **19**, 22 (2019).

19. Michel, R., Dugué, L. & Busch, N. A. Distinct contributions of alpha and theta rhythms to perceptual and attentional sampling. *Eur. J. Neurosci.* ejn.15154, 1–15 (2021).

20. Dugué, L., Marque, P. & VanRullen, R. Theta oscillations modulate attentional search performance periodically. *J. Cogn. Neurosci.* **27**, 945–958 (2015a).

21. Landau, A. N., Schreyer, H. M., van Pelt, S. & Fries, P. Distributed attention is implemented through theta-rhythmic gamma modulation. *Curr. Biol.* **25**, 2332–2337 (2015).

22. Fiebelkorn, I. C., Pinsk, M. A. & Kastner, S. A dynamic interplay within the frontoparietal network underlies rhythmic spatial attention. *Neuron* **99**, 842–853 (2018).

23. Helfrich, R. F. *et al.* Neural mechanisms of sustained attention are rhythmic. *Neuron* **99**, 854–865 (2018).

24. Haegens, S., Nácher, V., Luna, R., Romo, R., and Jensen, O. α-Oscillations in the monkey sensorimotor network influence discrimination performance by rhythmical inhibition of neuronal spiking. *Proc. Natl. Acad. Sci.* **108**, 19377–19382 (2011).

25. Buschman, T. J. & Miller, E. K. Serial, covert shifts of attention during visual search are reflected by the frontal eye fields and correlated with population oscillations. *Neuron* **63**, 386–396 (2009).

26. Voloh, B., Valiante, T. A., Everling, S. & Womelsdorf, T. Theta–gamma coordination between anterior cingulate and prefrontal cortex indexes correct attention shifts. *Proc. Natl. Acad. Sci. USA* **112**, 8457–8462 (2015).

27. Kienitz, R. *et al.* Theta rhythmic neuronal activity and reaction times arising from cortical receptive field interactions during distributed attention. *Curr. Biol.* **28**, 2377-2387.e5 (2018).

28. Fiebelkorn, I. C., Pinsk, M. A. & Kastner, S. The mediodorsal pulvinar coordinates the macaque fronto-parietal network during rhythmic spatial attention. *Nat. Commun.* **10**, 215 (2019).

29. Gaillard, C. *et al.* Prefrontal attentional saccades explore space rhythmically. *Nat. Commun.* **11**, 925 (2020).

30. Zareian, B. *et al.* Attention strengthens across-trial pre-stimulus phase coherence in visual cortex, enhancing stimulus processing. *Sci. Rep.* **10**, 4837 (2020).

31. Dugué, L., Beck, A.-A., Marque, P. & VanRullen, R. Contribution of FEF to attentional periodicity during visual search: a TMS study. *Eneuro* **6**, ENEURO.0357-18.2019 (2019).

32. Busch, N. A. & VanRullen, R. Spontaneous EEG oscillations reveal periodic sampling of visual attention. *Proc. Natl. Acad. Sci.* **107**, 16048–16053 (2010).

33. Fiebelkorn, I. C., Saalmann, Y. B. & Kastner, S. Rhythmic sampling within and between objects despite sustained attention at a cued location. *Curr. Biol.* **23**, 2553–2558 (2013).

34. Samaha, J., Bauer, P., Cimaroli, S. & Postle, B. R. Top-down control of the phase of alpha-band oscillations as a mechanism for temporal prediction. *Proc. Natl. Acad. Sci. USA* **112**, 8439–8444 (2015).

35. Chen, A., Wang, A., Wang, T., Tang, X. & Zhang, M. Behavioral oscillations in visual attention modulated by task difficulty. *Front. Psychol.* **8**, 1630 (2017).

36. Chen, A., Wang, A., Wang, T., Tang, X. & Zhang, M. The primary visual cortex modulates attention oscillation. *Acta Psychologica Sinica* **50**, 158 (2018).

37. Harris, A. M., Dux, P. E. & Mattingley, J. B. Detecting unattended stimuli depends on the phase of prestimulus neural oscillations. *J. Neurosci.* **38**, 3092–3101 (2018).

38. Peters, B., Kaiser, J., Rahm, B. & Bledowski, C. Object-based attention prioritizes working memory contents at a theta rhythm. *J. Exp. Psych. Gen.* **150**, 1250–1256 (2020).

39. Balestrieri, E., Ronconi, L. & Melcher, D. Shared resources between visual attention and visual working memory are allocated through rhythmic sampling. *Eur. J, Neurosci.* ejn.15264 (2021).

40. Plöchl, M., Fiebelkorn, I., Kastner, S. & Obleser, J. Attentional sampling of visual and auditory objects is captured by theta-modulated neural activity. *Eur. J. Neurosci.* ejn.15514 (2021).

41. Re, D., Inbar, M., Richter, C. G. & Landau, A. N. Feature-based attention samples stimuli rhythmically. *Curr. Biol.* **29**, 693-699.e4 (2019).

42. van der Werf, O. J., Ten Oever, S., Schuhmann, T. & Sack, A. T. No evidence of rhythmic visuospatial attention at cued locations in a spatial cuing paradigm, regardless of their behavioural relevance. *Eur. J. Neurosci.* ejn.15353 (2021).

43. van Es, M. W. J., Marshall, T. R., Spaak, E., Jensen, O. & Schoffelen, J. Phasic modulation of visual representations during sustained attention. *Eur. J. Neurosci.* ejn.15084 (2021).

44. Mayer, J. S. *et al.* Common neural substrates for visual working memory and attention. *NeuroImage* **36**, 441–453 (2007).

685 45. Fries, P., Reynolds, J. H., Rorie, A. E. & Desimone, R. Modulation of oscillatory neuronal
686 synchronization by selective visual attention. *Science* **291**, 1560–1563 (2001).

687 46. Klimesch, W., Schimke, H. & Pfurtscheller, G. Alpha frequency, cognitive load and memory
688 performance. *Brain Topogr.* **5**, 241–251 (1993).

689 47. Eckstein, M. P. Visual search: a retrospective. *J. Vis.* **11**, (2011).

690 48. Nakayama, K. & Martini, P. Situating visual search. *Vision Res.* **51**, 1526–1537 (2011).

691 49. Dugué, L., Marque, P. & VanRullen, R. Transcranial magnetic stimulation reveals attentional
692 feedback to area V1 during serial visual search. *PLoS ONE* **6**, e19712 (2011).

693 50. Palmer, J., Verghese, P. & Pavel, M. The psychophysics of visual search. *Vision Res.* **40**, 1227–
694 1268 (2000).

695 51. Treisman, A. Feature binding, attention and object perception. *Philos. Trans. R. Soc. Lond. B*
696 *Biol. Sci.* **353**(1373), 1295-1306 (1998).

697 52. Itti, L. & Koch, C. Computational modelling of visual attention. *Nat. Rev. Neurosci.* **2**, 194–203
698 (2001).

699 53. Deco, G., Pollatos, O., & Zihl, J. The time course of selective visual attention: theory and
700 experiments. *Vision Res.* **21**, (2002).

701 54. Senoussi, M. et al. *Theta oscillations shift towards optimal frequency for cognitive control*.
702 Preprint at http://biorxiv.org/lookup/doi/10.1101/2020.08.30.273706 (2020).

703 55. Busch, N. A., Dubois, J. & VanRullen, R. The phase of ongoing EEG oscillations predicts visual
704 perception. *J. Neurosci.* **29**, 7869–7876 (2009).

705 56. Mathewson, K. E., Gratton, G., Fabiani, M., Beck, D. M. & Ro, T. To see or not to see:
706 prestimulus alpha phase predicts visual awareness. *J. Neurosci.* **29**, 2725–2732 (2009).

707 57. Romei, V. *et al.* Spontaneous fluctuations in posterior α-band EEG activity reflect variability in
708 excitability of human visual areas. *Cereb. Cortex* **18**, 2010–2018 (2008).

709 58. Bernasconi, F., Manuel, A. L., Murray, M. M. & Spierer, L. Pre-stimulus beta oscillations within
710 left posterior sylvian regions impact auditory temporal order judgment accuracy. *Int. J.*
711 *Psychophysiol.* **79**, 244–248 (2011).

712 59. Dugué, L., Marque, P. & VanRullen, R. The phase of ongoing oscillations mediates the causal
713 relation between brain excitation and visual perception. *J. Neurosci.* **31**, 11889–11893 (2011).

714 60. Hanslmayr, S., Volberg, G., Wimber, M., Dalal, S. S. & Greenlee, M. W. Prestimulus oscillatory
715 phase at 7 hz gates cortical information flow and visual perception. *Curr. Biol.* **23**, 2273–2278
716 (2013).

717 61. Myers, N. E., Stokes, M. G., Walther, L. & Nobre, A. C. Oscillatory brain state predicts variability
718 in working memory. *J. Neurosci.* **34**, 7735–7743 (2014).

719 62. Spitzer, B., Blankenburg, F. & Summerfield, C. Rhythmic gain control during supramodal
720 integration of approximate number. *NeuroImage* **129**, 470–479 (2016).

721 63. Samaha, J., Gosseries, O. & Postle, B. R. Distinct oscillatory frequencies underlie excitability
722 of human occipital and parietal cortex. *J. Neurosci.* **37**, 2824–2833 (2017).

723 64. Benwell, C. S. Y., Coldea, A., Harvey, M. & Thut, G. Low pre-stimulus EEG alpha power
724 amplifies visual awareness but not visual sensitivity. *Eur. J. Neurosci.* ejn.15166 (2021).

725 65. Benwell, C. S. Y., Keitel, C., Harvey, M., Gross, J. & Thut, G. Trial-by-trial co-variation of pre-
726 stimulus EEG alpha power and visuospatial bias reflects a mixture of stochastic and deterministic
727 effects. *Eur. J. Neurosci.* **48**, 2566–2584 (2018).

728 66. Sauseng, P. *et al.* Are event-related potential components generated by phase resetting of brain
729 oscillations? A critical discussion. *Neuroscience* **146**, 1435–1444 (2007).

730 67. Makeig, S. *et al.* Dynamic brain sources of visual evoked responses. *Science* **295**, 690–694
731 (2002).

732 68. VanRullen, R. How to evaluate phase differences between trial groups in ongoing
733 electrophysiological signals. *Front. Neurosci.* **10**, (2016).

734 69. Fakche, C., VanRullen, R., Marque, P. & Dugué, L. Alpha phase-amplitude tradeoffs predict
735 visual perception. *eNeuro* ENEURO.0244-21.2022 (2022).

736 70. Veniero, D. *et al.* Top-down control of visual cortex by the frontal eye fields through oscillatory
737 realignment. *Nat. Commun.* **12**, 1757 (2021).

738 71. Wutz, A., Melcher, D., & Samaha, J. Frequency modulation of neural oscillations according to
739 visual task demands. *Proc. Natl. Acad. Sci.* **115**, 1346–1351 (2018).

740 72. Wolfe, J. M., Cave, K. R. & Franzel, S. L. Guided search: an alternative to the feature integration
741 model for visual search. *J. Exp. Psychol. Hum. Percept. Perform.* **15**, 419–433 (1989).

742 73. Treisman, A. M. & Gelade, G. A feature-integration theory of attention. *Cogn. Psychol.* **12**, 97-
743 136 (1980).

744 74. Dugué, L., Merriam, E. P., Heeger, D. J. & Carrasco, M. Specific visual subregions of TPJ
745 mediate reorienting of spatial attention. *Cereb. Cortex* **28**, 2375–2390 (2017).

746 75. Dugué, L., Merriam, E. P., Heeger, D. J. & Carrasco, M. Differential impact of endogenous and
747 exogenous attention on activity in human visual cortex. *Sci. Rep.* **10**, 21274 (2020).

748 76. Kastner, S. & Pinsk, M. A. Visual attention as a multilevel selection process. *Cogn. Affect.*
749 *Behav. Neurosci.* **4**, 483–500 (2004).

750 77. de Graaf, T. A. & Duecker, F. No effects of rhythmic visual stimulation on target discrimination:
751 An online alpha entrainment experiment. *Eur. J. Neurosci.* ejn.15483 (2021).

752 78. Liu, T., Pestilli, F. & Carrasco, M. Transient attention enhances perceptual performance and
753 fmri response in human visual cortex. *Neuron* **45**, 469–477 (2005).

754 79. Fernández, A. & Carrasco, M. Extinguishing exogenous attention via transcranial magnetic
755 stimulation. *Curr. Biol.* **30**, 4078-4084 (2020).

756 80. Pestilli, F., Carrasco, M., Heeger, D. J. & Gardner, J. L. Attentional enhancement via selection
757 and pooling of early sensory responses in human visual cortex. *Neuron* **72**, 832–846 (2011).

758 81. Ling, S. & Carrasco, M. When sustained attention impairs perception. *Nat. Neurosci.* **9**, 1243–
759 1245 (2006).

760 82. Pestilli, F., Ling, S. & Carrasco, M. A population-coding model of attention's influence on
761 contrast response: estimating neural effects from psychophysical data. *Vision Res.* **49**, 1144–1153
762 (2009).

763 83. Nakayama, K. & Mackeben, M. Sustained and transient components of focal visual attention.
764 *Vision Res.* **29**, 1631–1647 (1989).

765 84. Buschman, T. J. & Miller, E. K. Top-down versus bottom-up control of attention in the prefrontal
766 and posterior parietal cortices. *Science* **315**, 1860–1862 (2007).

767 85. Wolfe, J. M. & Horowitz, T. S. Five factors that guide attention in visual search. *Nat. Hum.*
768 *Behav.* **1**, (2017).

769 86. van Kerkoerle, T. *et al.* Alpha and gamma oscillations characterize feedback and feedforward
770 processing in monkey visual cortex. *Proc. Natl. Acad. Sci. USA* **111**, 14332–14341 (2014).

771 87. Michalareas, G. *et al.* Alpha-beta and gamma rhythms subserve feedback and feedforward
772 influences among human visual cortical areas. *Neuron* **89**, 384–397 (2016).

773 88. Brainard, D. H. The psychophysics toolbox, *Spat. Vis.* **10**, 433-436 (1997).

774 89. Pelli, D. G. The VideoToolbox software for visual psychophysics: transforming numbers into
775 movies, *Spat. Vis.* **10**, 437-442 (1997).

90. Kleiner, M., Brainard, D. & Pelli, D. What's new in Psychtoolbox-3? *Perception 36 ECVP Abstract Supplement.* 89 [HTML] (2007).

91. Watson, A. B. & Pelli, D. G. Quest: A Bayesian adaptive psychometric method. *Percept. Psychophys.* **33**, 113–120 (1983).

92. Delorme, A. & Makeig, S. EEGLAB: an open source toolbox for analysis of single-trial EEG dynamics including independent component analysis. *J. Neurosci. Methods* **134**, 9–21 (2004).

93. Cohen, M. X. *Analyzing Neural Time Series Data: Theory And Practice*. (MIT press, 2014).

94. Stouffer, S. A., Suchman, E. A., Devinney, L. C., Star, S. A. & Williams, Jr, R. M. *Studies in social psychology in World War II: the American soldier. Vol. 1, Adjustment during army life.* (Princeton, NJ: Princeton University Press, 1949).

95. Benjamini, Y. & Hochberg, Y. Controlling the false discovery rate: a practical and powerful approach to multiple testing. *Journal of the Royal statistical society: series B (Methodological)* **57**, 289–300 (1995).

96. VanRullen, R. Perceptual Rhythms. in *Stevens' Handbook of Experimental Psychology and Cognitive Neuroscience* (ed. Wixted, J. T.) 1–44 (John Wiley & Sons, Inc., 2018).

Acknowledgements

This project has received funding from the Agence Nationale de la Recherche (ANR) - Deutsche Forschungsgemeinschaft (DFG) programme (grant agreement No J18P08ANR00 – Laura Dugué), the ANR programme (grant agreement No ANR-19-NEUC-0004 – Rufin VanRullen), and the Université de Paris IDEX doctoral programme (grant No J18I08IDEX13 – Garance Merholz).

Author contributions

Conceived and designed the experiments: LD, RV. Performed the experiments: LD. Analyzed the data: GM, LG, LD. Prepared the figures: GM. Reviewed and edited the figures: GM, LG, LD. Wrote the first draft of the manuscript: GM. Reviewed and edited the manuscript: GM, LG, LD, RV.

Additional Information

Competing Interests: The authors have declared that no competing interests exist.